



A rapid and accurate computer vision system for measuring the volume of axi-symmetric natural products based on cubic spline interpolation

Joko Siswantoro^{*}, Endah Asmawati, Muhammad Z.F.N. Siswantoro

Department of Informatics Engineering, Faculty of Engineering, University of Surabaya, Jl. Kali Rungkut Tengilis, Surabaya, 60293, Indonesia

ARTICLE INFO

Keywords:

Computer vision
Cubic spline interpolation
Volume measurement
Axi-symmetric natural products

ABSTRACT

The volume contains prominent information used to evaluate the visual quality of natural products and can be measured using a computer vision system. The computer vision system provides an alternative method for measuring the volume of natural products, especially for axi-symmetric natural products. The volume of axi-symmetric natural products can be obtained using integral for the volume of solid of revolution by rotating the boundary curve of the upper half object cross-section. This study proposes a computer vision system for measuring the volume of axi-symmetric natural products based on cubic spline interpolation. A piecewise cubic polynomial was constructed using cubic spline interpolation to approximate the boundary curve of the upper half object cross-section based on the boundary points of the object extracted from the image of the object. The polynomial was integrated to obtain the volume of the object. The experimental result reveals that the proposed system achieved an accurate volume measurement result with a mean absolute relative error of 1.03% compared to the water displacement method result.

1. Introduction

Volume measurement has several applications in producing and processing natural products, such as sorting, grading, planting strategy, and plant phenotyping (Siswantoro et al., 2014b; Su et al., 2017; Wang and Li, 2014). Volume and weight can also be used to predict produce density, which plays an important role in determining the chemical composition and detecting defects such as frost damage (Chopin et al., 2017). Measuring the volume of natural products is not a simple task. Generally, a natural product is an irregularly shaped object whose volume cannot be calculated directly using a standard mathematical formula.

The water displacement method based on Archimedes' principle is an accurate conventional method for measuring volume. However, this method is time-consuming and may be inaccurate for the porous object that can absorb water. Furthermore, it can be considered destructive for some products (Siswantoro et al., 2014b; Wang and Nguang, 2007). A modern approach to measuring the volume of natural products is performed using a computer vision system. This approach is nondestructive and more efficient compared to the water displacement method. Several volume measurement methods have been proposed to measure the volume of natural products by employing either a 3D or 2D computer

vision system. The methods extracted some features from the image of the measured object and then used the features to predict volume (Moreda et al., 2009).

In measuring the volume of natural products, the 3D computer vision system required more than one image captured from several views. Generally, the captured images were used to perform 3D object reconstruction. The volume of the measured object was calculated from the reconstructed 3D object either by calculating the number of voxels or using a mathematical formula, as proposed by Chalidabhongse et al. (2006), Lee et al. (2006), Goñi et al. (2007), Castillo-Castaneda and Turchiuli (2008), Zhang et al. (2016), Chopin et al. (2017), Concha-Meyer et al. (2018), Jadhav et al. (2019), Liong et al. (2019), Mon and ZarAung (2020), Li et al. (2021), and Zavala de Paz et al. (2021). Siswantoro et al. (2014b) have proposed a 3D computer vision system to measure the volume of irregularly shaped food products without performing 3D object reconstruction. The proposed system employed Monte Carlo integration with heuristic adjustment on a 3D bounding box for the product in real-world coordinate. The bounding box was constructed from the captured images using a method proposed by Siswantoro et al. (2013). Even though the volume measurement method using 3D computer vision system could be used to measure the volume of arbitrarily shaped natural product and achieved a good accuracy, the

^{*} Corresponding author.

E-mail address: joko_siswantoro@staff.ubaya.ac.id (J. Siswantoro).

method required high computational cost and time.

Wang and Li (2014), Su et al. (2017), Nyalala et al. (2019), and Okinda et al. (2020) have proposed a 3D computer vision system for volume measurement by employing a color and depth camera to capture the images of the measured object. The system proposed by Wang and Li (2014) captured color and depth images from a view only, while that one proposed by Su et al. (2017), Nyalala et al. (2019), and Okinda et al. (2020) required color and depth images from several views. The system proposed by Wang and Li (2014) and Su et al. (2017) constructed a 3D model from color and depth images. Furthermore, the number of voxels in the model and some mathematical formulas were employed to approximate the volume. On the other hand, Nyalala et al. (2019) and Okinda et al. (2020) extracted some 2D and 3D features from the captured image to predict the volume using some regression models.

The 2D computer vision system for volume measurement only requires an image of the measured object captured from a particular view. The captured image is then processed to obtain a silhouette of the object that represents the object cross-section. In general, the 2D computer vision system is used to measure the volume of axi-symmetric objects. A natural product is categorized as an axi-symmetric object if it has a rotation axis, such as egg, lemon, and orange (Siswanto et al., 2014a). An axi-symmetric natural product can be considered as a solid of revolution obtained by rotating half of its cross-section around its rotating axis. Therefore, the volume of axi-symmetric natural products can be calculated using a method for calculating the volume of a solid of revolution as long as the equation of the boundary curve of the production cross-section is known (Weir et al., 2010).

Sabliov et al. (2002), Du and Sun (2006), and Wang and Nguang (2007) have proposed methods to measure the volume of axi-symmetric agriculture products from an image by approximating the boundary curve of the product cross-section with a piecewise continuous linear function. With this approach, the volume of the product was obtained by the sum of the right circular conical frustum volume. Huynh et al. (2020) have proposed a real-time volume estimation method for slender axi-symmetric fruits/vegetables by modifying the method proposed by Sabliov et al. (2002) and dividing the cross-section of the measured object into eight segments. The upper and lower segments were assumed to be conical cross-sections, while the rest were conical frustum cross-sections. With this assumption, the volume of the product was obtained by summing the volume of cones and conical frustums.

A slightly different volume approximation method has been proposed by Bridge et al. (2007), Koc (2007), Zhou et al. (2009), Khojastehnazhand et al. (2019), and Widiarsi et al. (2019). They approximated the volume of the axi-symmetric product as the sum of circular disk (thin circular cylinder) volume by assuming the boundary curve of product cross-section is a piecewise constant function. Khojastehnazhand et al. (2009), Khojastehnazhand et al. (2010), and Omid et al. (2010) have proposed volume estimation methods by replacing the circular disk with an elliptical disk. Both disk and conical frustum approaches require a lot of points on the boundary of the object cross-section to obtain good accuracy. It could happen since a linear function or a constant function was employed to represent the boundary curve of the product cross-section, which is generally a nonlinear function. In addition, the method proposed by Sabliov et al. (2002), Bridge et al. (2007), and Koc (2007) were not fully automatic.

The nonlinear approach was also used in the volume measurement of axi-symmetric objects, as proposed by Soltani et al. (2015), Vivek Venkatesh et al. (2015), Ziaratban et al. (2017), Siswanto et al. (2017), Jana et al. (2020), and Nyalala et al. (2021). Soltani et al. (2015) proposed a method to predict volume based on Pappus's theorem. The volume was obtained by determining the area and centroid of half the object cross-section and employing Pappus's second centroid theorem. Vivek Venkatesh et al. (2015) treated the boundary of the object cross-section as one of the following shapes: circle, ellipse, or parabolic. The volume was calculated using a formula based on the shape of the boundary. Ziaratban et al. (2017) and Siswanto et al. (2017) used an

artificial neural network (ANN) model to predict volume based on 1D and 2D features extracted from the object cross-section. Nyalala et al. (2021) achieved the best prediction for the volume of tomatoes using a support vector regression (SVR) model with a radial basis function (RBF) kernel, based on 1D and 2D features extracted from the object cross-section. A deep neural network (DNN) model was also used to predict the volume of carrots based on five cross-section diameters and the length, as reported by Örnek and Kahramanlı Örnek (2021). However, the input features of the DNN model were extracted manually using a vernier caliper and a ruler. Jana et al. (2020) approximated the boundary of object cross-section using 10th order polynomial obtained using interpolation based on some point in the boundary. The polynomial was then integrated to get the volume of the object using an integral for the volume of solid revolution. Although most proposed methods claim to have good accuracy, they are only used to predict the volume of one particular type of object except the method proposed by Vivek Venkatesh et al. (2015).

Image segmentation is an essential step in volume measurement using computer vision. Segmentation aims to localize the object in an image. The accuracy of volume measurement is highly dependent on the result of segmentation. In some previous studies, a common method for image segmentation was automatic thresholding based on the Otsu method (Otsu, 1979). Some morphological operators were also employed after thresholding to improve the segmentation result, as reported by Badaró et al. (2021) and Oliveira et al. (2021).

Siswanto and Asmawati (2016) have proposed a new framework for measuring the volume of axi-symmetric natural products based on cubic spline interpolation using a computer vision system. Cubic spline interpolation was used to approximate the boundary curve of object cross-section by constructing a piecewise continuous cubic polynomial. The volume of products was then obtained by integrating the polynomial. Cubic spline interpolation provides a better approximation for a nonlinear smooth function than a piecewise continuous linear function. Furthermore, by employing cubic spline interpolation, the oscillatory nature of high degree polynomial, which usually occurs in ordinary polynomial interpolation, can be avoided (Burden et al., 2009). However, the proposed framework was not implemented to measure the volume of real axi-symmetric natural products. Therefore, the performance of the proposed framework in measuring the volume of real natural products needs to be investigated.

This study aims to propose a rapid and accurate computer vision system for measuring the volume of axi-symmetric natural products based on cubic spline interpolation. The overall process in the proposed system is based on the volume measurement framework proposed by Siswanto and Asmawati (2016). Three types of axi-symmetric natural products were used to measure the performance of the proposed system, including eggs, lemons, and oranges. The rest of the paper is organized as follows. Section two describes the materials and methods used in this study. Results and discussion are explained in section three. Finally, conclusions are drawn in section four.

2. Materials and methods

2.1. Natural products samples

An experiment was performed to measure the performance of the proposed computer vision system using three types of axi-symmetric natural products. The samples of natural products used in the experiment were 30 eggs, ten lemons, and ten oranges. All samples were collected randomly from traditional and modern markets in Surabaya, Indonesia. The volume of each product was measured using the proposed system three times, and the average of these three measurements was considered as the approximation volume. For comparison, the volume of each product was also measured using the water displacement method based on Archimedes' principle to obtain the exact volume.

2.2. Computer vision system

A computer vision system consisting of hardware and software was developed to implement the volume measurement framework proposed by Siswanto and Asmawati (2016). The hardware used to develop the system was a camera, an illumination source, a computer, and a container box. A Logitech HD Webcam C270h with resolution HD 720p (720 px × 1280 px) was used to acquire the image of the measured object. The camera was connected to a portable computer with a 2.20 GHz Intel Core 2 Duo processor, 2 GB RAM, and Windows 7 operating system using the USB cable. For the illumination source, the system employed two 5 Watt portable LED bulbs connected to the computer using the USB cable to obtain the electricity source. The camera, bulbs, and measured object were contained in a black painted closed container box with dimensions 50 cm × 50 cm × 50 cm to ensure that the system has constant illumination intensity. The arrangement of the hardware and measured object are shown in Fig. 1.

The computer was equipped with software to perform a series of processes for volume measurement, including image acquisition, pre-processing, segmentation, and volume approximation. All processes in the software can be seen in Fig. 2. The software was developed using Visual C++ 2010 with open-source computer vision library OpenCV 231 (Bradski and Kaehler, 2008) and numerical analysis and data processing library ALGLIB 3.10.0 Free Edition (Bochkanov and Bystritsky). A simple and user-friendly user interface was developed to facilitate users who do not have a computer vision background in measuring the volume of axi-symmetric natural produce, as shown in Fig. 3.

2.3. Image acquisition

The computer vision system acquired the image of the measured object using a camera from the top view with a black background. The black background was chosen since the eggs, lemons, and oranges have a different surface color from black. In this condition, the measured object could be easily separated from its background by using image thresholding in the segmentation process. The measured object was located under the camera at about 50 cm.

The image was acquired in RGB (Red Green Blue) color space with a dimension of 640 pixels × 480 pixels and a resolution of 96 dpi both in vertical and horizontal directions. The image was then saved in JPEG format for the following process. In addition, the system could also use an image that has been saved in a JPEG file. The examples of the acquired image are shown in Fig. 4.

2.4. Pre-processing

Pre-processing aims to produce a grayscale image that will be used in segmentation. This step consisted of color transformation and noise reduction. According to Siswanto et al. (2014b), the segmentation process for the image of natural products could be easily performed in HSV (Hue Saturation Value) color space. Therefore, the acquired image

was firstly transformed from RGB color space to HSV color space using a transformation as shown in Eqs. (1)–(3). The example of a transformed image in HSV color space is shown in Fig. 5.

$$H = \begin{cases} 60 \left(\frac{G - B}{R - \min(R, G, B)} \right), & \max(R, G, B) = R \\ 60 \left(\frac{B - R}{G - \min(R, G, B)} + 2 \right), & \max(R, G, B) = G \\ 60 \left(\frac{R - G}{B - \min(R, G, B)} + 4 \right), & \max(R, G, B) = B \end{cases} \quad (1)$$

$$S = \begin{cases} \frac{\max(R, G, B) - \min(R, G, B)}{\max(R, G, B)}, & \max(R, G, B) \neq 0 \\ 0, & \max(R, G, B) = 0 \end{cases} \quad (2)$$

$$V = \max(R, G, B) \quad (3)$$

As can be seen in, Fig. 5, the measured object could be easily separated from its background in the S and V channels. Therefore, images in the S and V channels were used to construct a grayscale image Gr. The intensity of every pixel in Gr was obtained from the weighted sum of pixel intensity in the S and V channels, as shown in Eq. (4). The weight of each channel in Eq. (4) was heuristically determined to obtain the optimum segmentation result.

$$Gr = 0.3S + 0.7V \quad (4)$$

Finally, a 15 × 15 Gaussian filter (Gonzalez and Woods, 2002) was applied to reduce noise in the grayscale image resulting from the camera. The examples of preprocessing results are shown in Fig. 6.

2.5. Segmentation

Segmentation is a step to separate the object from its background in the grayscale image. This step produced a binary image consisting of white pixels and black pixels. Every pixel in the grayscale image was clustered into a white pixel with binary value 1 for the object and a black pixel with binary value 0 for the background.

The system employed image thresholding to perform segmentation. The threshold value T was automatically determined using the Otsu method (Otsu, 1979). A pixel in the grayscale image with pixel intensity less than T was transformed into a black pixel in the binary image, otherwise to a white pixel. After thresholding, a few object pixels were transformed into the black background and vice versa. Two morphological operators, opening and closing operators with a 5 × 5 ellipse kernel, were used to solve this segmentation problem. The examples of segmentation results can be seen in Fig. 7. From Figs. 4 and 7, it can be seen that the object in the binary image is close to the object in the original image. This fact shows that the Otsu method combined with opening and closing operators is appropriate for the segmentation step in the proposed system.

2.6. Volume approximation

In this step, the volume of the measured object is extracted from the binary image. This step consists of a series of sub-steps, including image cropping, real-world coordinate axes construction, boundary points determination, scale factor determination, cubic spline interpolation, and integration. The detail for every sub-step is explained in the following sub-sections.

2.6.1. Image cropping

Before image cropping, the segmented image was rotated such that the major axis of the object is parallel to the horizontal axis of the image coordinate. This process was used to ensure the object's rotation axis was parallel to the horizontal axis of the image coordinate. By employing image rotation, the object could be placed in arbitrary

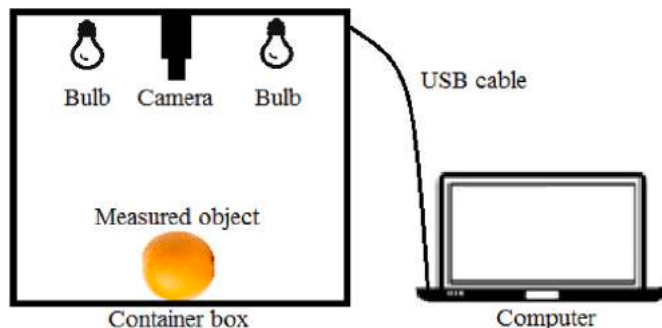


Fig. 1. The arrangement of the hardware.

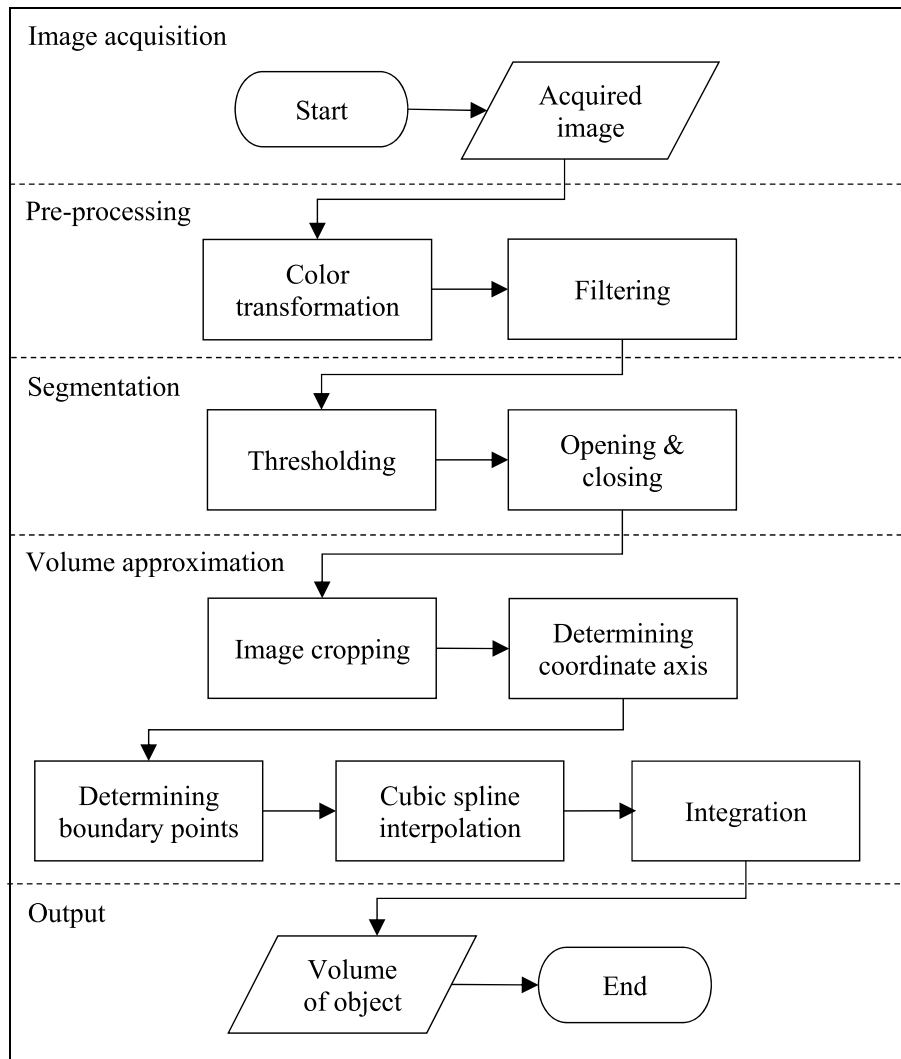


Fig. 2. The detailed process of the software for the proposed system.

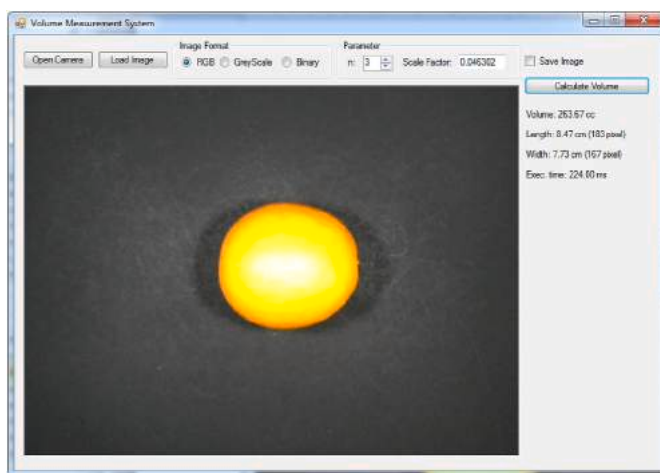


Fig. 3. User interface for measuring the volume of axi-symmetric natural produce.

direction during image acquisition.

Image cropping was started by determining an axis-aligned minimum bounding rectangle of the object. The bounding rectangle was

determined by finding the minimum and maximum coordinates of white pixels in the binary image both in the horizontal and vertical directions. The binary image was then cropped according to the bounding rectangle. Fig. 8 shows examples of the bounding rectangle and the cropped binary image.

2.6.2. Real-world coordinate axes construction

The system used an integral for the volume of solid revolution to approximate the volume of the measured object. The integral was calculated in a 2D real-world coordinate system. Therefore, the coordinate axes of the 2D real-world coordinate system needed to be constructed. Let M be the height of the cropped binary image. Two-dimensional real-world coordinate axes were constructed using the following assumptions:

1. The cross-section of the measured object, which is parallel to the rotation axis of the measured object, is located on the xy-plane.
2. The left-most object pixel is located on the y axis.
3. The rotation axis of the measured object is located on $[M/2]^{\text{th}}$ row of the cropped binary image and coincides with the x-axis, where $[M/2]$ is the smallest integer greater than or equal to $M/2$. Fig. 9 shows the example of constructed real-world coordinate axes.

2.6.3. Boundary points determination

To approximate the boundary curve of the upper half object cross-

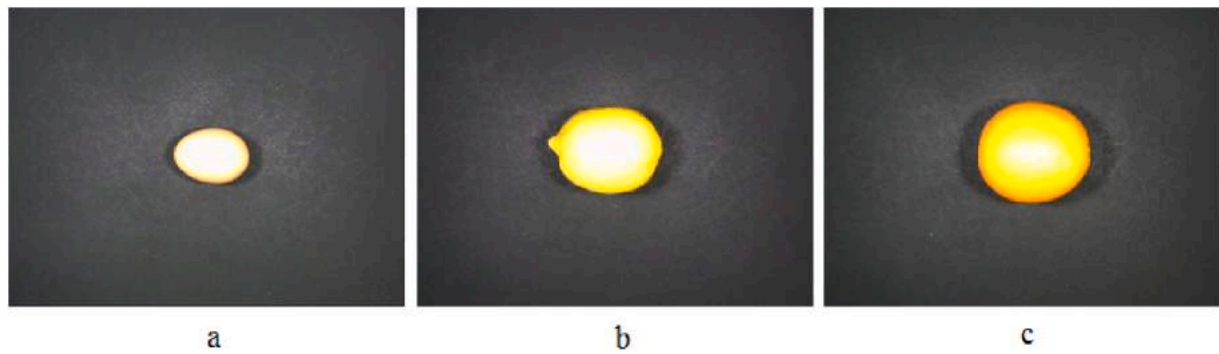


Fig. 4. The examples of acquired images: (a) egg, (b) lemon, and (c) orange.

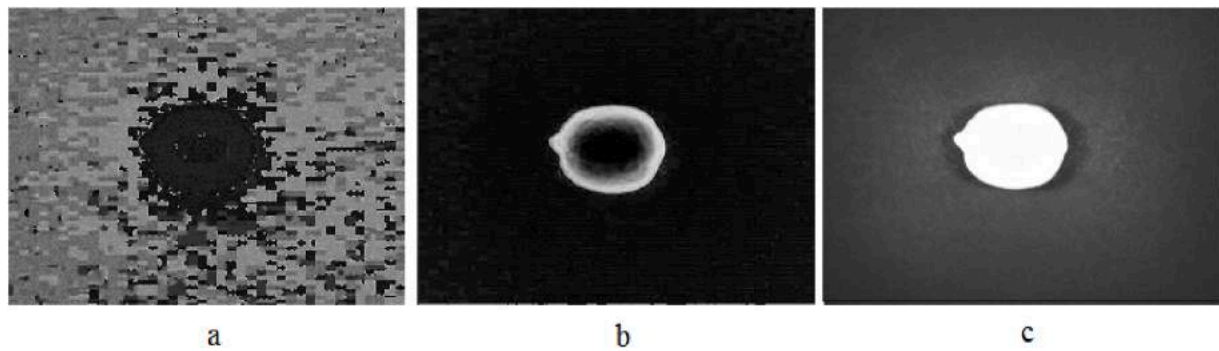


Fig. 5. The example of a transformed image in HSV color space: (a) H channel, (b) S channel, and (c) V channel.

section using cubic spline interpolation, a subset of pixels on the boundary of the upper half object cross-section consisting of $n+1$ pixels needed to be determined. The value of n was chosen depending on the

shape of the boundary curve. Since the curvature variation for every type of natural product was different, the value of n would also be different for every type of natural product.

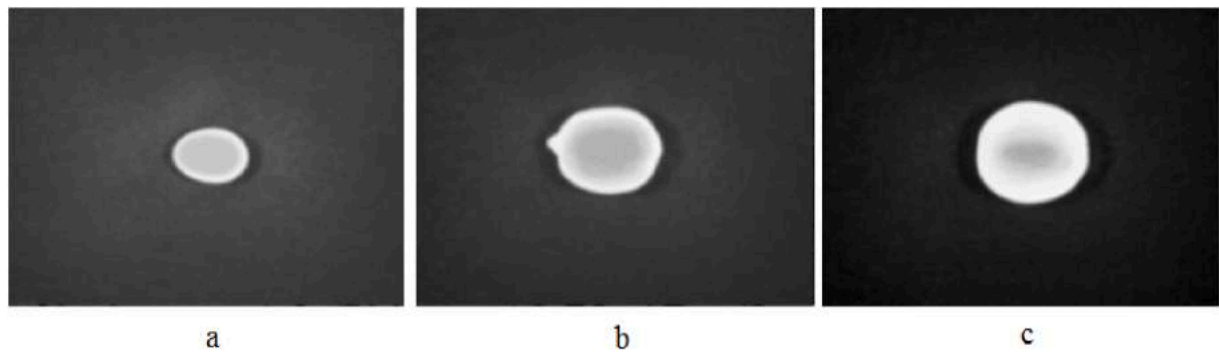


Fig. 6. The examples of preprocessing results: (a) egg, (b) lemon, and (c) orange.

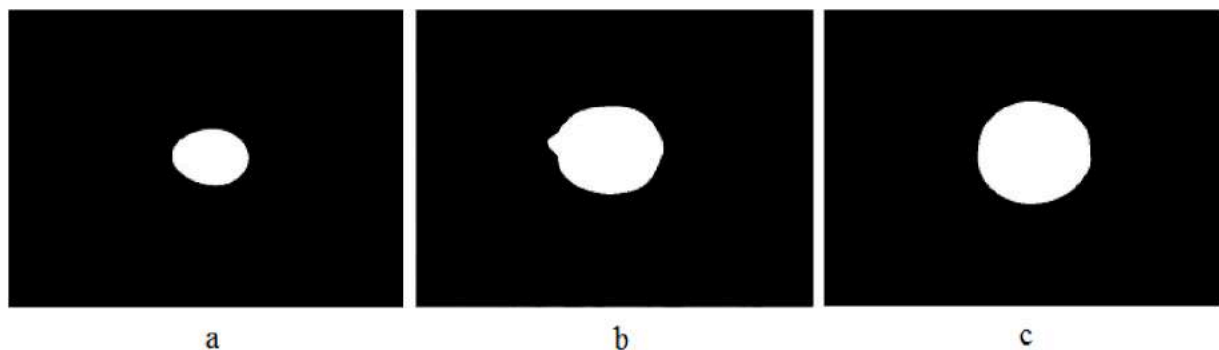


Fig. 7. The examples of segmentation results: (a) egg, (b) lemon, and (c) orange.

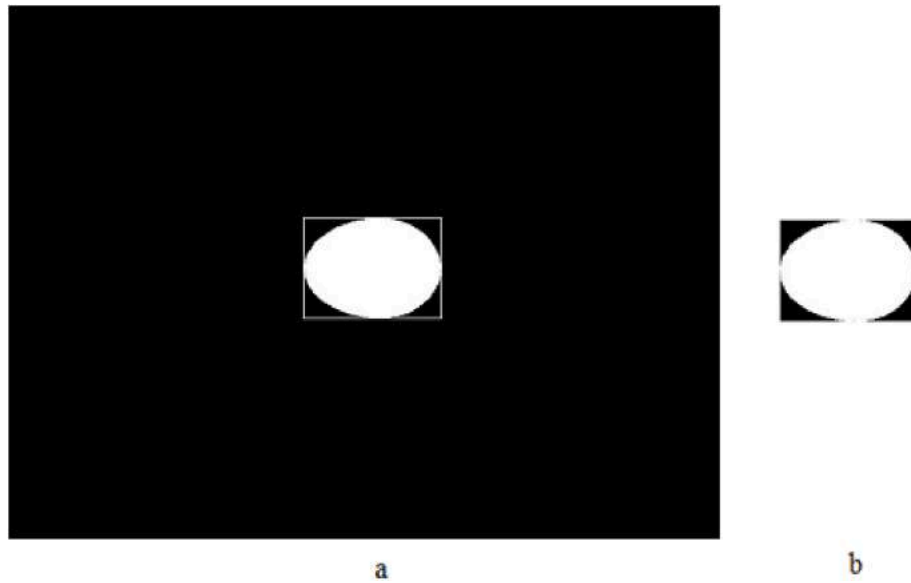


Fig. 8. The example of the bounding rectangle and cropped binary image.

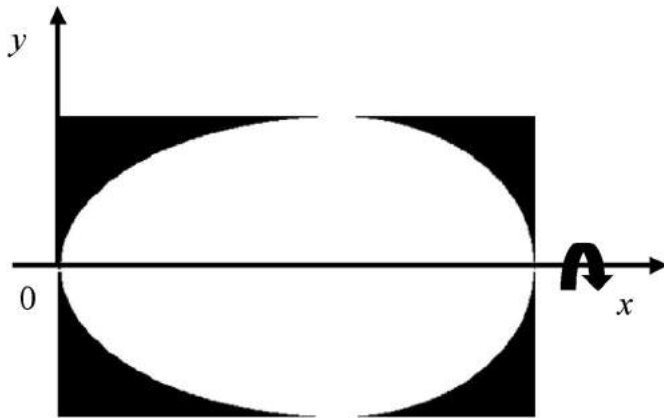


Fig. 9. The example of constructed real-world coordinate axes.

It can be observed in Fig. 7 that the boundary curve of the egg cross-section had a slight curvature variation. Every point on the boundary curve of the egg cross-section had almost the same curvature. On the other hand, the boundary curve of the lemon cross-section had a greater variation in curvature than the egg. On the left part of the lemon, the curve had a slight curvature, but the curvature then increased rapidly, and then near the center part of the lemon, it again decreased. In contrast, the boundary curve of the orange cross-section was almost similar to the egg. Based on these facts, a preliminary experiment was performed to determine the number of selected pixels. The values of n used in the experiment were 2, 3, and 4 for egg and lemon, and 5, 10, 15, 20, and 25 for lemon.

The experiment was conducted according to the following steps:

1. Choose a random sample from each type of natural product.
2. Capture the image of the sample.
3. Process the image to obtain a cropped binary image B.
4. Choose a value of n from $\{2, 3, 4\}$ or $\{5, 10, 15, 20, 25\}$.
5. Let N be the width of the cropped binary image, divide the interval $[0, N]$ into n equal length subintervals with boundary point $x_i = iN/n$, $i = 0, 1, \dots, n$.

6. Determine the coordinate of points on the boundary of the upper half object cross-section at $x = x_i$ to obtain $n + 1$ points (x_i, y_i) , $i = 0, 1, \dots, n$, where

$$y_i = \begin{cases} \sum_{j=1}^M B(j, 1)/2, & i = 0 \\ \sum_{j=1}^M B(j, iN/n)/2, & i = 2, 3, \dots, n \end{cases} \quad (5)$$

7. Construct a piecewise cubic polynomial using cubic spline interpolation from (x_i, y_i) , $i = 0, 1, \dots, n$ to approximate the boundary curve of the upper half object cross-section.
8. Repeat step 4 until 7 such that an appropriate boundary curve approximation is obtained.

2.6.4. Cubic spline interpolation

Before being used to construct a piecewise cubic polynomial for volume approximation, the coordinates of $n + 1$ points on the boundary curve of the upper half of the object cross-section (x_i, y_i) , $i = 0, 1, \dots, n$ were transformed from the image coordinate system into the 2D real-world coordinate system using the following equations.

$$X_i = kx_i, \quad Y_i = ky_i, \quad i = 0, 1, \dots, n \quad (6)$$

Here, k is a scale factor used to convert length in the image coordinate system into the 2D real-world coordinate system. The image of a reference object with a known length was captured using the system to obtain the value of k . The value of k was equal to the ratio between the length of the reference object in the real-world coordinate system and its length in the image coordinate system.

Suppose $y = f(x)$, $0 \leq x \leq kN$ is the exact boundary curve of the upper half of the measured object cross-section. A piecewise cubic polynomial $S(x)$ was then constructed from (X_i, Y_i^2) , $i = 0, 1, \dots, n$, using cubic spline interpolation to approximate $[f(x)]^2$. The polynomial $S(x)$ was denoted as $S_j(x)$ on subinterval $[X_j, X_{j+1}]$ for each $j = 0, 1, 2, \dots, n - 1$ as in the following equation.

$$S_j(x) = a_j + b_j(x - X_j) + c_j(x - X_j)^2 + d_j(x - X_j)^3, \quad (7)$$

for $x \in [X_j, X_{j+1}]$

The steps used to determine the value of coefficients a_j, b_j, c_j, d_j are provided in Appendix.

2.6.5. Integration

By assuming that a measured object is an axi-symmetric object, then the volume of the measured object can be obtained using the integral for the volume of a solid revolution, as in the following equation (Weir et al., 2010).

$$V = \int_0^{kN} \pi [f(x)]^2 dx \quad (8)$$

Where V is the volume of the measured object, $y = f(x)$, $0 \leq x \leq kN$ is the boundary curve of the object cross-section, k is the scale factor, and N is the width of the cropped binary image. Since $[f(x)]^2$ was approximated by $S(x)$, then by using Eq. (7) the integral in Eq. (8) can be expressed as,

$$\begin{aligned} V &= \int_0^{kN} \pi S(x) dx \\ &= \pi \sum_{j=0}^{n-1} \int_{X_j}^{X_{j+1}} S_j(x) dx \\ &= \pi \sum_{j=0}^{n-1} \int_{X_j}^{X_{j+1}} \left(a_j + b_j(x - X_j) + c_j(x - X_j)^2 + d_j(x - X_j)^3 \right) dx \\ &= \pi \sum_{j=0}^{n-1} \left(a_j x + \frac{b_j}{2}(x - X_j)^2 + \frac{c_j}{3}(x - X_j)^3 + \frac{d_j}{4}(x - X_j)^4 \right) \Big|_{X_j}^{X_{j+1}} \\ &= \pi \sum_{j=0}^{n-1} \left(a_j(X_{j+1} - X_j) + \frac{b_j}{2}(X_{j+1} - X_j)^2 + \frac{c_j}{3}(X_{j+1} - X_j)^3 + \frac{d_j}{4}(X_{j+1} - X_j)^4 \right) \\ &= \pi \sum_{j=0}^{n-1} \left(a_j \Delta X_j + \frac{b_j}{2} \Delta X_j^2 + \frac{c_j}{3} \Delta X_j^3 + \frac{d_j}{4} \Delta X_j^4 \right) \end{aligned} \quad (9)$$

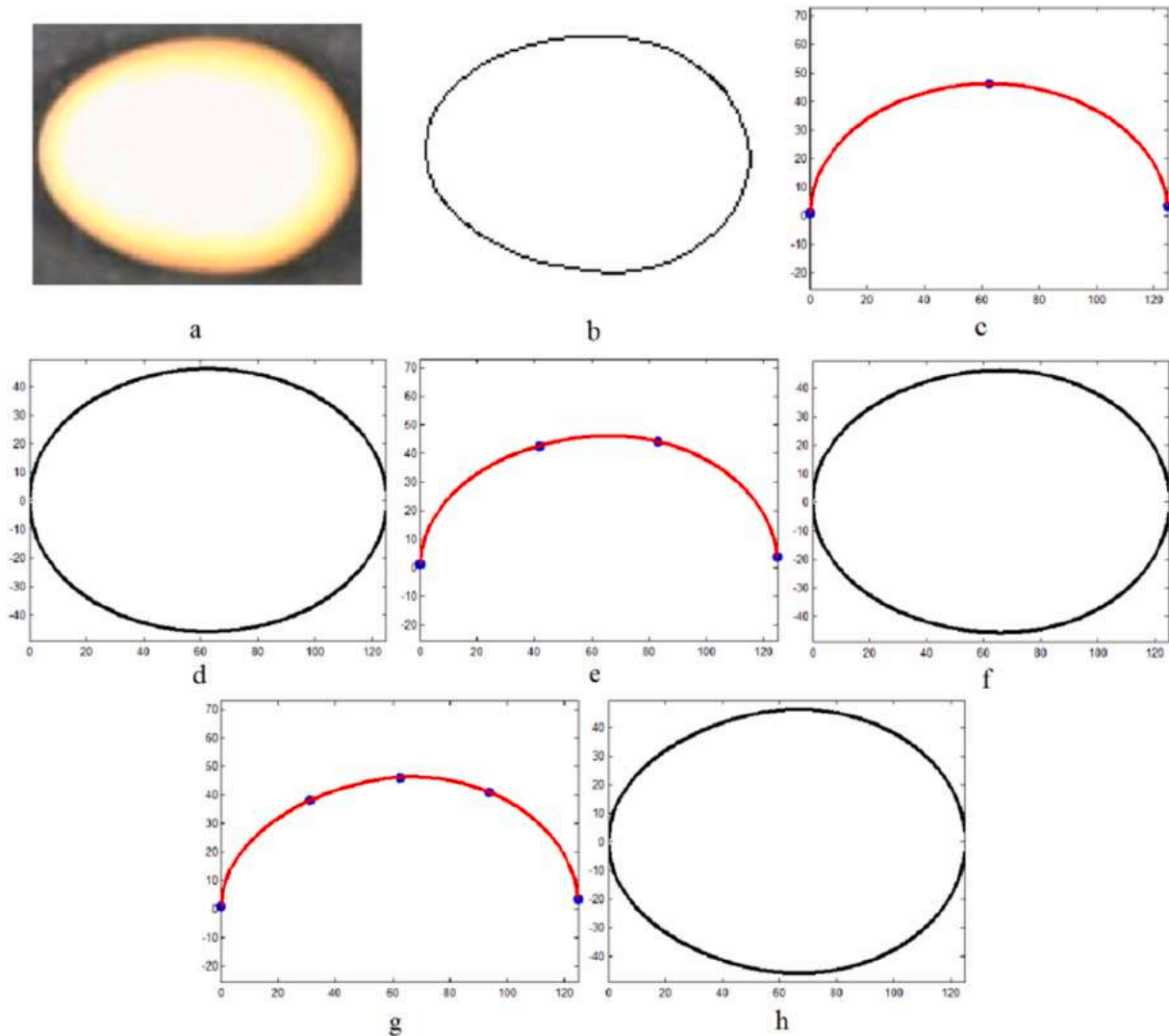


Fig. 10. (a) The acquired image of egg; (b) egg cross section; (c), (e), (g) the results of cubic spline interpolation; (d), (f), (h) the approximation of egg cross section for $n = 2$, $n = 3$, $n = 4$, respectively.

where $\Delta X_j = X_{j+1} - X_j, j = 0, 1, 2, \dots, n-1$.

2.7. Evaluation

The performance of the proposed system was evaluated using a volume measurement accuracy. The accuracy was measured by comparing the approximation volume measured using the proposed system and the exact volume measured using the water displacement method. The absolute relative error (ARE) was calculated from the approximation volume (V_A) and the exact volume (V_E) for every product

using Eq. (10).

$$ARE(\%) = \frac{|V_E - V_A|}{V_E} \times 100 \quad (10)$$

The linear relationship between the approximation volume and the exact volume was evaluated using the correlation coefficient (R) and the coefficient of determination (R^2). In addition, the paired t -test was used to examine whether the mean difference between the two measurement results was zero.

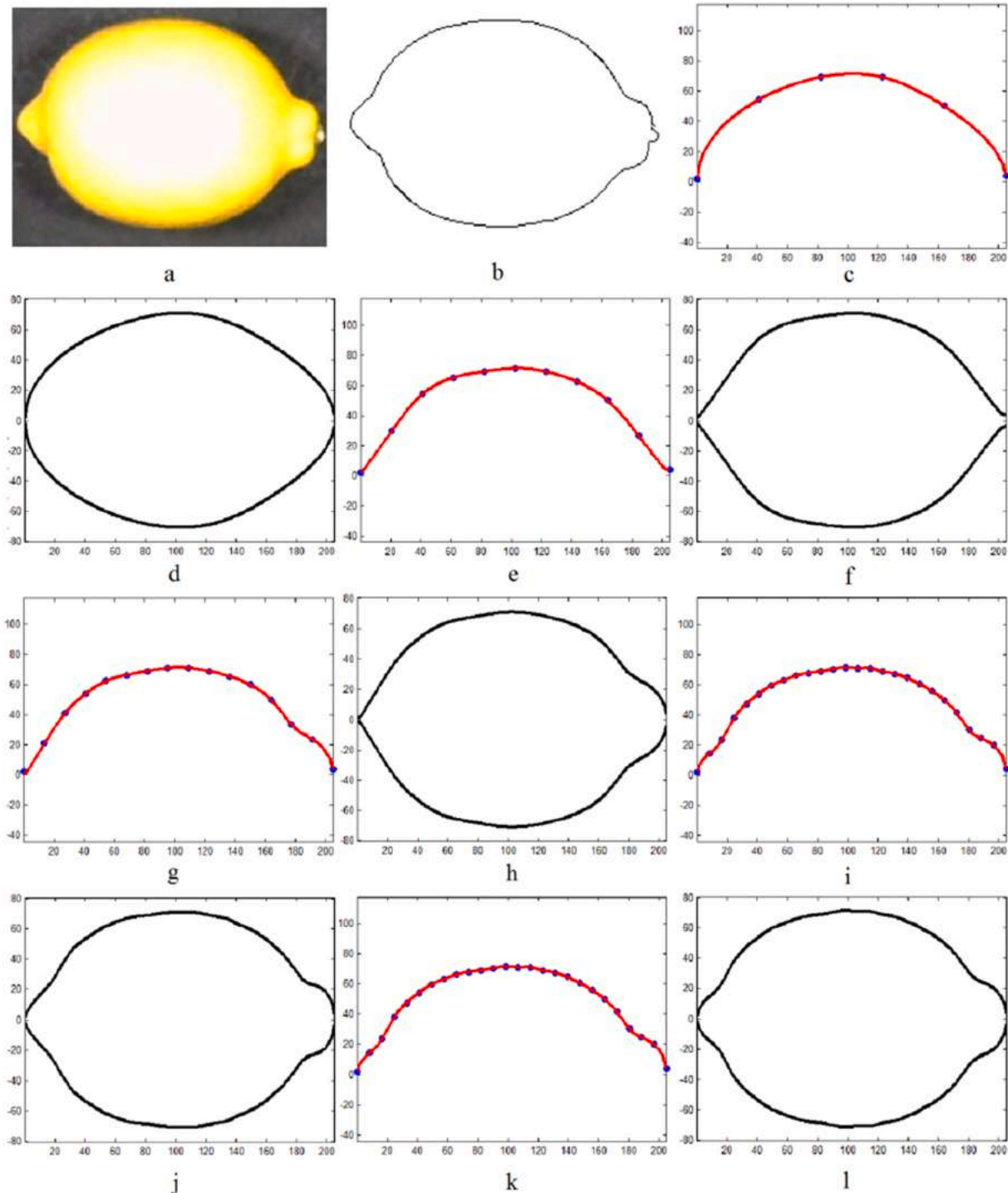


Fig. 11. (a) The acquired image of lemon; (b) lemon cross section; (c), (e), (g), (i), (k) the results of cubic spline interpolation; (d), (f), (h), (j), (l) the approximation of lemon cross section for $n = 5, n = 10, n = 15, n = 20, n = 25$, respectively.

3. Results and discussion

The preliminary experiment results to determine the number of points on the boundary of the upper half of the object cross-section used for cubic spline interpolation are depicted in Fig. 10, Fig. 11, and Fig. 12. As can be seen in Fig. 10, the approximations of the egg cross-section using cubic spline interpolation were different from the original egg cross-section extracted from the acquired image (Fig. 10 (b)) for $n = 2$ (Fig. 10 (d)) and $n = 3$ (Fig. 10 (f)). However, for $n = 4$ (Fig. 10(h)), the approximation was similar to the original one.

For lemon, cubic spline interpolation needed $n = 25$ (Fig. 11 (l)) to produce an approximation of the lemon cross-section that is similar to the original lemon cross-section. Unlike egg and lemon, cubic spline interpolation only needed $n = 3$ to obtain an appropriate approximation of the orange cross-section. Increasing the value of n did not affect the approximation result. As can be seen in Fig. 12 (f) and (h), there was no difference between the approximation of the orange cross-section with $n = 3$ and $n = 4$. Therefore, the number of points on the boundary of the upper half of the egg, lemon, and orange cross-section used in the experiment were set to 5 (or $n = 4$), 26 (or $n = 25$), and 4 (or $n = 3$), respectively.

The volume measurement result measured using the proposed system and the water displacement method together with its ARE summarized in Table 1. From Table 1, it can be seen that, on average, volume

measurement results measured using the proposed system and the water displacement method were close to each other for all samples, which were 115.27 cm^3 and 115.23 cm^3 , respectively. The proposed system produced the mean ARE of 1.03% for all samples, with minimum and maximum ARE being 0.00% and 2.39%, respectively, if compared to the water displacement method. Overall, ARE was less than 2% for 86% of samples. This result shows that the proposed system has high volume measurement accuracy. Furthermore, the standard deviation of ARE was 0.79% for all samples. Therefore, it can be inferred that the proposed system produces high precision volume measurement results. The proposed system had different mean ARE for every type of natural product. The smallest mean ARE was achieved in measuring the volume of eggs ($0.94\% \pm 0.69\%$), followed by lemons ($1.02\% \pm 0.79\%$) and oranges ($1.30\% \pm 0.86\%$). These results occur since the egg had an almost perfect axis-symmetric shape than lemon and orange. In addition, all egg samples had minor variations in shape compared to lemon and orange.

The volume measurement result of the proposed system was highly correlated with the volume measurement results of the water displacement method. For all samples, the correlation coefficient (R) of these two volume measurement results was 0.9997. This result shows that the volume measurement result of the proposed system had an excellent linear relationship with the volume measurement results of the water displacement method, as shown in Fig. 13. Since all R^2 s were greater than 0.99 (see Fig. 13), it can be concluded that more than 99%

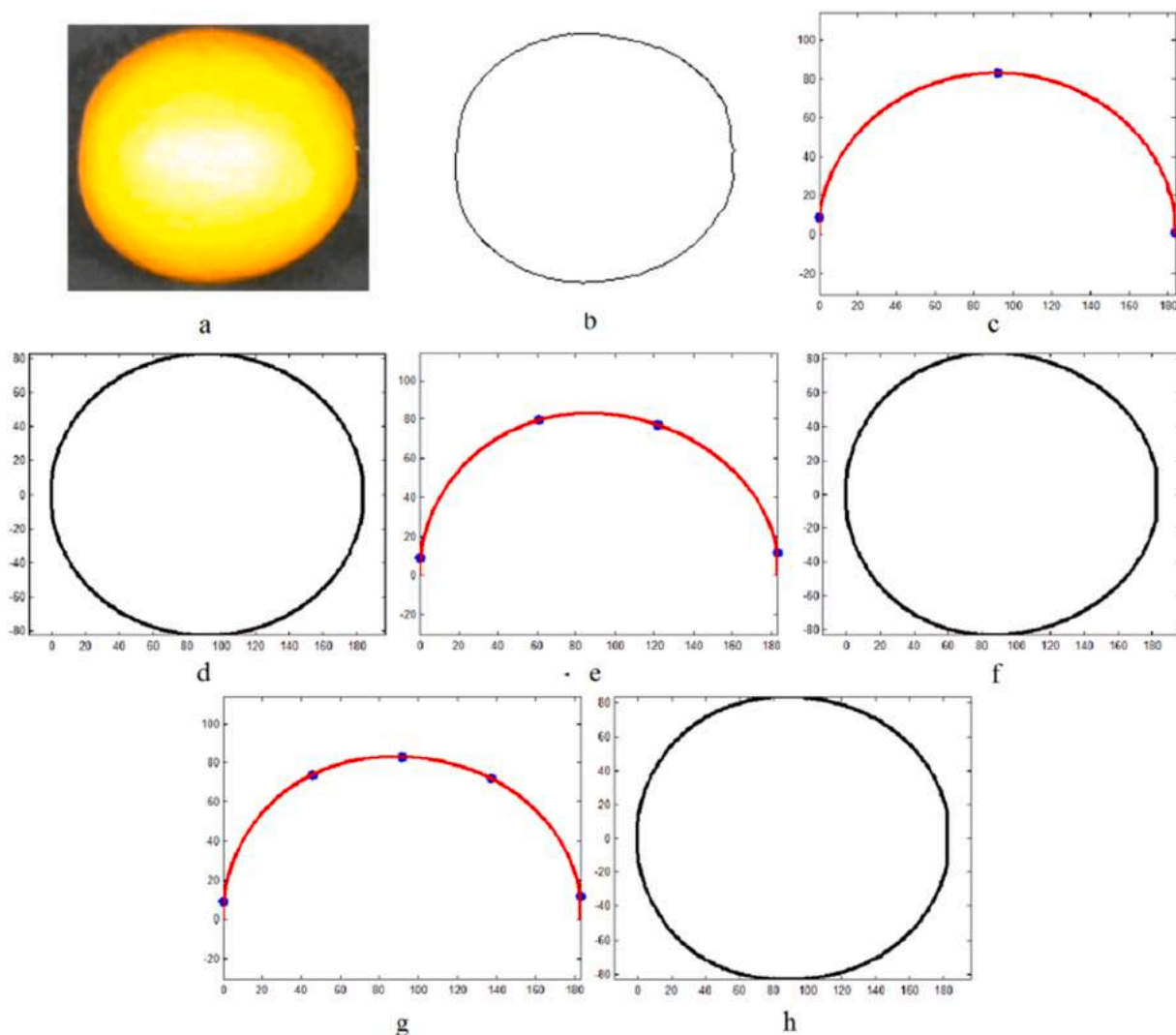
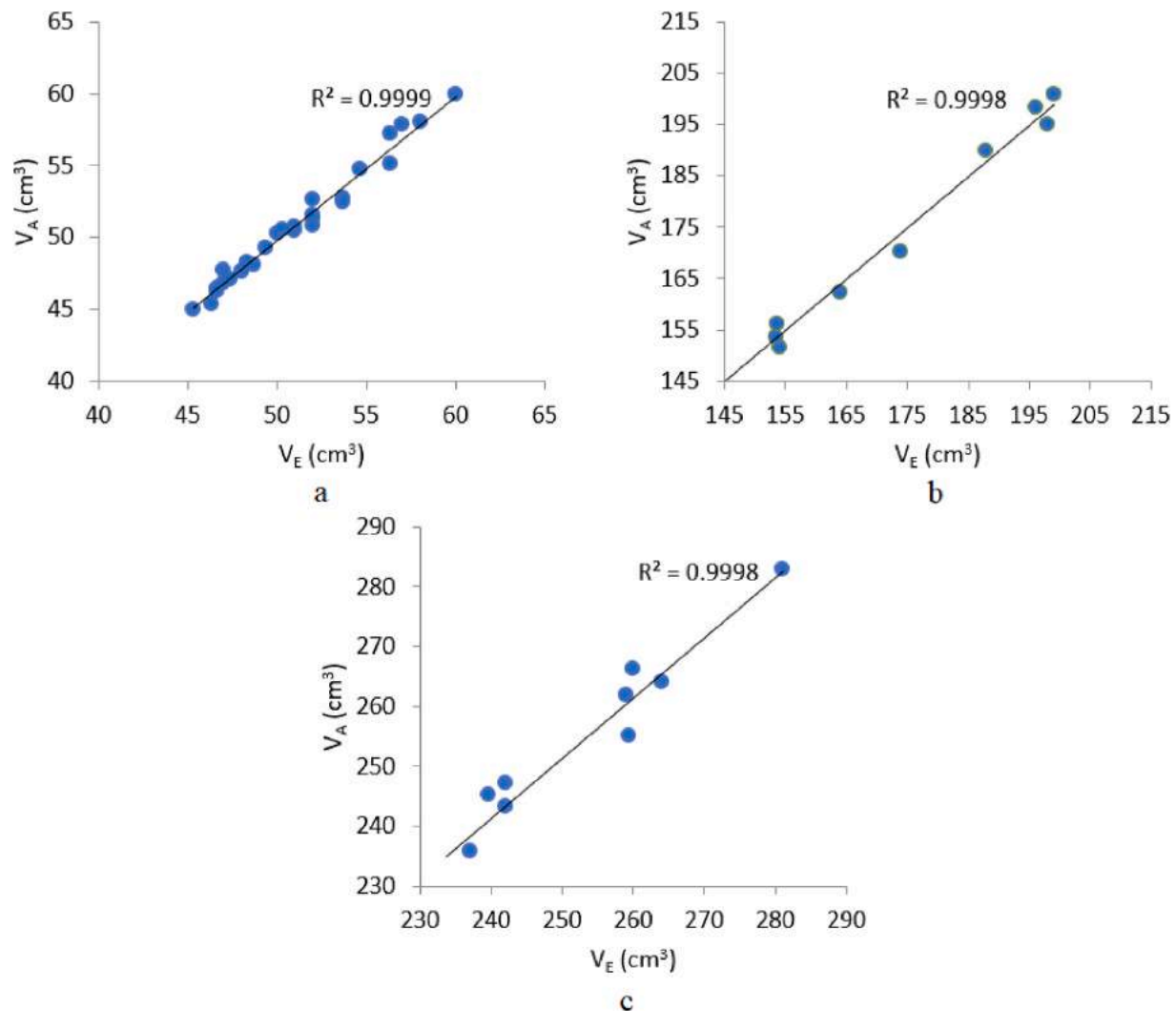


Fig. 12. (a) The acquired image of orange; (b) orange cross section; (c), (e), (g) the results of cubic spline interpolation; (d), (f), (h) the approximation of orange cross section for $n = 2$, $n = 3$, $n = 4$, respectively.

Table 1

The summary of volume measurement results measured using the proposed system and the water displacement method.

Natural produce	Number of samples	V_A (cm ³)				V_E (cm ³)				ARE (%)			
		Mean	Min	Max	Std. dev.	Mean	Min	Max	Std. dev.	Mean	Min	Max	Std. dev.
Egg	30	50.56	44.97	60.00	4.05	50.79	45.33	60.00	3.94	0.94	0.00	2.22	0.69
Lemon	10	171.51	142.60	198.95	21.17	172.53	145.33	199.00	21.14	1.02	0.00	1.92	0.79
Orange	10	253.18	229.67	282.88	15.95	251.77	233.67	281.00	15.15	1.30	0.00	2.39	0.86
All samples	50	115.27	44.97	282.88	85.03	115.33	45.33	281.00	84.56	1.03	0.00	2.39	0.74

**Fig. 13.** The linear relationship between the volume measurement results of the proposed system (V_A) and the water displacement method (V_E): (a) egg, (b) lemon, and (c) orange.

variation of the volume measurement result of the water displacement method can be explained by the volume measurement result proposed system using a linear relationship.

For further analysis, the paired t -test was used to show no significant difference between the volume measurement result of the proposed system and the water displacement method. The test was performed with a level of significance $\alpha = 0.05$ and the following hypothesis,

$$H_0 : \mu_1 - \mu_2 = 0$$

$$H_1 : \mu_1 - \mu_2 \neq 0$$

where μ_1 and μ_2 are mean volume measurement results of the proposed system and the water displacement method, respectively. The result of the paired t -test is tabulated in Table 2.

Table 2The result of paired t -test.

Paired difference		t	d. f.	95% confidence interval for the mean difference		p -value
Mean (cm ³)	Std. dev. (cm ³)			Lower bound	Upper bound	
-0.062	2.0248	-0.2165	49	-0.6375	0.5134	0.8295

As can be seen in Table 2, the mean paired difference between the two-volume measurement results was -0.062 with a 95% confidence interval $[-0.6375, 0.5134]$. This fact shows that the mean paired difference between the two-volume measurement results was close to zero.

Table 3

The summaries of the absolute relative errors from all measurement method.

Authors	Method	ARE (%)	
		Mean	Std. dev.
Sabliov et al. (2002), Du and Sun (2006), Wang and Nguang (2007)	Conical frustum	1.67	1.05
Bridge et al. (2007), Koc (2007), Zhou et al. (2009), Khojastehnazhand et al. (2019), Widiastri et al. (2019)	Disk	1.63	1.05
Soltani et al. (2015)	Pappus's theorem	1.57	1.58
Vivek Venkatesh et al. (2015)	Sphere, ellipsoid, paraboloid	10.63	6.62
Ziaratban et al. (2017)	ANN	2.42	2.33
Siswanto et al. (2017)	ANN	1.80	2.15
Huynh et al. (2020)	Cone and conical frustum	30.53	6.90
Jana et al. (2020)	10th order polynomial interpolation	2.84	3.80
Nyalala et al. (2021)	RBF SVR	2.17	2.43
This study	Cubic spline interpolation	1.03	0.74

Furthermore, since the p -value of the test was 0.8295 (greater than α), then there is insufficient evidence at the level of 0.05 to reject H_0 . Therefore, it can be concluded that there is no significant difference between the volume measurement result of the proposed system and the water displacement method.

The proposed system is faster than the water displacement method in terms of computational time. The proposed system only required about 0.20 s until 0.25 s in approximating the volume of a sample, while the water displacement method required about 60 s. This required time can be reduced by employing a rapid industrial camera and high-speed computer to acquire and process images. Therefore, there is a possibility to further implement the proposed system into an automated visual inspection system for natural produce grading based on the size in the industry.

For comparison, the volume of all samples was also measured using some existing volume measurement methods based on a single image. All volume measurement results were compared with the volume obtained with the water displacement method by calculating the absolute relative errors. The summaries of the absolute relative errors from all measurement methods are tabulated in Table 3. As shown in Table 3, the proposed system achieved the lowest mean absolute relative error compared to other methods. This result indicates that the proposed

system has better accuracy in measuring the volume of axi-symmetric natural products than other methods. In addition, the proposed system also produced the lowest standard deviation of absolute relative error compared to other methods. This result shows that the proposed system is more precise than other methods.

4. Conclusions

In this study, a computer vision system was proposed to measure the volume of axi-symmetric natural produces. An image of the measured object was captured from the top view and then processed to obtain a binary image. Some boundary points of the measured object were extracted from the binary image and used to construct a piecewise cubic polynomial using cubic spline interpolation. The polynomial was then used to calculate the volume of the measured object using the integral for the volume of solid of revolution. Fifty samples of axi-symmetric natural products consisting of 30 eggs, ten lemons, and ten oranges were used to validate the proposed system. The experimental results indicate that the proposed system produces a high accuracy volume measurement result with a mean absolute relative error of 1.03% compared to the volume measurement result of the water displacement method. In addition, the statistical analysis result shows that the volume measurement result of the proposed system is not significantly different from the volume measurement result of the water displacement method. For future studies, the application of the proposed system in a visual inspection system for natural product grading based on size needs to be investigated. Furthermore, more samples used to validate the volume measurement model need to be considered to improve the robustness of the model.

Credit author statement

Joko Siswanto: Conceptualization, Methodology, Software, Investigation, Writing - Review & Editing, Project administration, Funding acquisition. **Endah Asmawati:** Conceptualization, Validation, Formal analysis, Resources. **Muhammad Z. F. N. Siswanto:** Software, Validation, Investigation, Visualization, Editing, Resources.

Acknowledgments

The authors would like to thank University of Surabaya for providing facilities and financial support under Grant no.006/Lit/LPPM-01/FT/IV/2016.

Appendix

The steps used to determine the value a_j, b_j, c_j, d_j in Eq. (7) are as follows (Burden et al., 2009).

1. For $j = 0, 1, 2, \dots, n-1$ do steps 2 and 3:
2. Set $a_j = Y_j^2$.
3. Set $\Delta X_j = X_{j+1} - X_j$.
4. For $j = 1, 2, \dots, n-1$ do step 5:
5. Set $\alpha_j = \frac{3}{\Delta X_j} (a_{j+1} - a_j) - \frac{3}{\Delta X_{j-1}} (a_j - a_{j-1})$.
6. Set $l_0 = 0, \mu_0 = 0, z_0 = 0$.
7. For $j = 1, 2, \dots, n-1$ do steps 8, 9, and 10:
8. Set $l_j = 2(X_{j+1} - X_j) - \Delta X_{j-1} \mu_{j-1}$.
9. Set $\mu_j = \frac{\Delta X_j}{l_j}$.
10. Set $z_j = \frac{a_j - \Delta X_{j-1} z_{j-1}}{l_j}$.
11. Set $l_n = 0, \mu_n = 0, z_n = 0$.
12. For $j = n-1, n-2, \dots, 0$ do steps 13, 14, and 15:
13. Set $c_j = z_j - \mu_j c_{j+1}$.
14. Set $d_j = \frac{c_{j+1} - c_j}{3\Delta X_j}$.

$$15. \text{ Set } b_j = \frac{a_{j+1} - a_j}{\Delta X_j} - \Delta X_j \frac{c_{j+1} - 2c_j}{3}$$

References

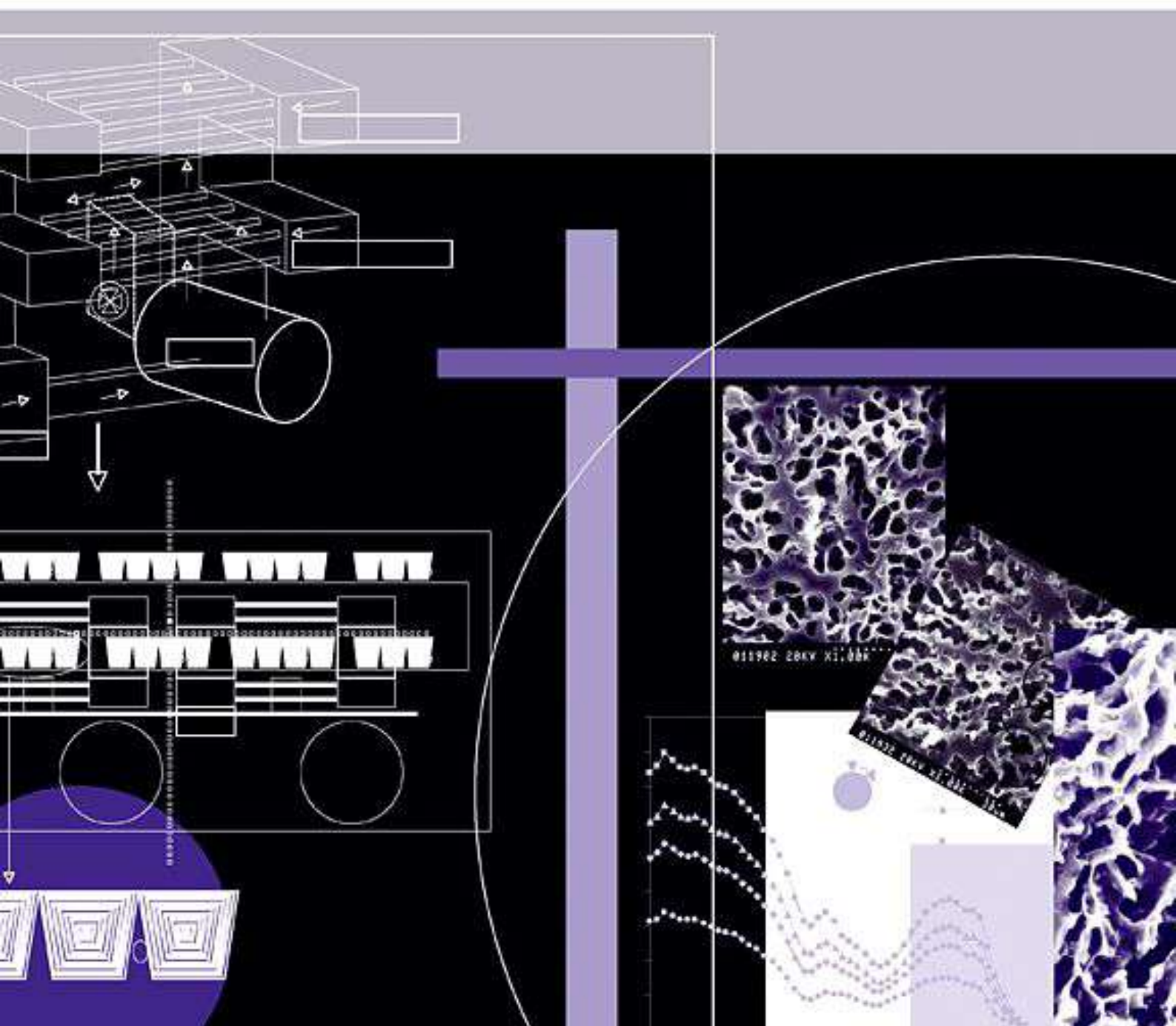
- Badaró, A.T., de Matos, G.V., Karaziack, C.B., Viotto, W.H., Barbin, D.F., 2021. Automated method for determination of cheese meltability by computer vision. *Food Anal. Methods* 14 (12), 2630–2641. <https://doi.org/10.1007/s12161-021-02094-1>.
- Bochkanov, S., Bystritsky, V., Alglib. <http://www.alglib.net/>.
- Bradski, G., Kaehler, A., 2008. *Learning OpenCV: Computer Vision with the OpenCV Library*. O'Reilly Media, Inc., Sebastopol, CA.
- Bridge, E.S., Boughton, R.K., Aldredge, R.A., Harrison, T.J.E., Bowman, R., Schoech, S.J., 2007. Measuring egg size using digital photography: testing Hoyt's method using Florida Scrub-Jay eggs. *Field Ornithol* 78 (1), 109–116.
- Burden, R.L., Faires, J.D., Reynolds, A.C., 2009. *Numerical Analysis*, ninth ed. Brooks Cole, Boston, MA.
- Castillo-Castaneda, E., Turchiuli, C., 2008. Volume estimation of small particles using three-dimensional reconstruction from multiple views. In: Elmoataz, A., Lezoray, O., Nouboud, F., Mammass, D. (Eds.), *Image and Signal Processing*. Springer Berlin/Heidelberg, pp. 218–225. https://doi.org/10.1007/978-3-540-69905-7_25.
- Chalidabhongse, T., Yimyan, P., Sirisomboon, P., 2006. 2D/3D vision-based mango's feature extraction and sorting. In: 9th International Conference on Control, Automation, Robotics and Vision, ICARCV, pp. 1–6, 6.
- Chopin, J., Laga, H., Miklavcic, S.J., 2017. A new method for accurate, high-throughput volume estimation from three 2D projective images. *Int. J. Food Prop.* 20 (10), 2344–2357. <https://doi.org/10.1080/10942912.2016.1236814>.
- Concha-Meyer, A., Eifert, J., Wang, H., Sanglay, G., 2018. Volume estimation of strawberries, mushrooms, and tomatoes with a machine vision system. *Int. J. Food Prop.* 21 (1), 1867–1874. <https://doi.org/10.1080/10942912.2018.1508156>.
- Du, C.-J., Sun, D.-W., 2006. Estimating the surface area and volume of ellipsoidal ham using computer vision. *J. Food Eng.* 73 (3), 260–268. <https://doi.org/10.1016/j.jfoodeng.2005.01.029>.
- Goñi, S.M., Puris, E., Salvadori, V.O., 2007. Three-dimensional reconstruction of irregular foodstuffs. *J. Food Eng.* 82 (4), 536–547. <https://doi.org/10.1016/j.jfoodeng.2007.03.021>.
- Gonzalez, R.C., Woods, R.E., 2002. *Digital Image Processing*, second ed. Prentice Hall.
- Huynh, T., Tran, L., Dao, S., 2020. Real-time size and mass estimation of slender axis-symmetric fruit/vegetable using a single top view image. *Sensors* 20 (18), 5406.
- Jadhav, T., Singh, K., Abhyankar, A., 2019. Volumetric estimation using 3D reconstruction method for grading of fruits. *Multimed. Tool. Appl.* 78 (2), 1613–1634. <https://doi.org/10.1007/s11042-018-6271-3>.
- Jana, S., Parekh, R., Sarkar, B., 2020. A De novo approach for automatic volume and mass estimation of fruits and vegetables. *Optik* 200, 163443. <https://doi.org/10.1016/j.jleo.2019.163443>.
- Khojastehnazhand, M., Mohammadi, V., Minaei, S., 2019. Maturity detection and volume estimation of apricot using image processing technique. *Sci. Hortic.* 251, 247–251. <https://doi.org/10.1016/j.scienta.2019.03.033>.
- Khojastehnazhand, M., Omid, M., Tabatabaeefar, A., 2009. Determination of orange volume and surface area using image processing technique. *Int. Agrophys.* 23, 237–242.
- Khojastehnazhand, M., Omid, M., Tabatabaeefar, A., 2010. Determination of tangerine volume using image processing methods. *Int. J. Food Prop.* 13 (4), 760–770. <https://doi.org/10.1080/10942910902894062>.
- Koc, A.B., 2007. Determination of watermelon volume using ellipsoid approximation and image processing. *Postharvest Biol. Technol.* 45 (3), 366–371. <https://doi.org/10.1016/j.postharvbio.2007.03.010>.
- Lee, D.J., Xu, X., Eifert, J., Zhan, P., 2006. Area and volume measurements of objects with irregular shapes using multiple silhouettes. *Opt. Eng.* 45 (2), 027202.
- Li, H., Sun, Q., Liu, S., Shi, Y., 2021. A novel tomato volume measurement method based on machine vision. *Teh. Vjesn.* 28 (5), 1674–1680.
- Liong, S.-T., Gan, Y.-S., Huang, Y.-C., 2019. Automatic surface area and volume prediction on ellipsoidal ham using deep learning. *J. Food Process. Eng.* 42 (5), e13093 <https://doi.org/10.1111/jfpe.13093>.
- Mon, T., ZarAug, N., 2020. Vision based volume estimation method for automatic mango grading system. *Biosyst. Eng.* 198, 338–349. <https://doi.org/10.1016/j.biosystemseng.2020.08.021>.
- Moreda, G.P., Ortiz-Cañavate, J., García-Ramos, F.J., Ruiz-Altisent, M., 2009. Nondestructive technologies for fruit and vegetable size determination – a review. *J. Food Eng.* 92 (2), 119–136. <https://doi.org/10.1016/j.jfoodeng.2008.11.004>.
- Nyalala, I., Okinda, C., Chao, Q., Mecha, P., Korohou, T., Yi, Z., Nyalala, S., Jiayu, Z., Chao, L., Kunjie, C., 2021. Weight and volume estimation of single and occluded tomatoes using machine vision. *Int. J. Food Prop.* 24 (1), 818–832. <https://doi.org/10.1080/10942912.2021.1933024>.
- Nyalala, I., Okinda, C., Nyalala, L., Makange, N., Chao, Q., Chao, L., Yousaf, K., Chen, K., 2019. Tomato volume and mass estimation using computer vision and machine learning algorithms: cherry tomato model. *J. Food Eng.* 263, 288–298. <https://doi.org/10.1016/j.jfoodeng.2019.07.012>.
- Okinda, C., Sun, Y., Nyalala, I., Korohou, T., Opiyo, S., Wang, J., Shen, M., 2020. Egg volume estimation based on image processing and computer vision. *J. Food Eng.* 283, 110041. <https://doi.org/10.1016/j.jfoodeng.2020.110041>.
- Oliveira, M.M., Cerqueira, B.V., Barbon, S., Barbin, D.F., 2021. Classification of fermented cocoa beans (cut test) using computer vision. *J. Food Compos. Anal.* 97, 103771. <https://doi.org/10.1016/j.jfca.2020.103771>.
- Omid, M., Khojastehnazhand, M., Tabatabaeefar, A., 2010. Estimating volume and mass of citrus fruits by image processing technique. *J. Food Eng.* 100 (2), 315–321. <https://doi.org/10.1016/j.jfoodeng.2010.04.015>.
- Örnek, M.N., Kahramanlı Örnek, H., 2021. Developing a deep neural network model for predicting carrots volume. *J. Food Meas. Char.* 15 (4), 3471–3479. <https://doi.org/10.1007/s11694-021-00923-9>.
- Otsu, N., 1979. A threshold selection method from gray-level histograms. *Systems, Man and Cybernetics, IEEE Transactions on* 9 (1), 62–66. <https://doi.org/10.1109/tsmc.1979.4310076>.
- Sabliov, C.M., Boldor, D., Keener, K.M., Farkas, B.E., 2002. Image processing method to determine surface area and volume of axis-symmetric agricultural products. *Int. J. Food Prop.* 5 (3), 641–653.
- Siswanto, J., Asmawati, E., 2016. A new framework for measuring volume of axisymmetric food products using computer vision system based on cubic spline interpolation. In: *Science in Information Technology (ICSITech), 2016 2nd International Conference on*. IEEE, pp. 74–78.
- Siswanto, J., Hilman, M.Y., Widiari, M., 2017. Computer vision system for egg volume prediction using backpropagation neural network. In: *IOP Conference Series: Materials Science and Engineering*, vol. 273, 012002. <https://doi.org/10.1088/1757-899x/245/1/012002>.
- Siswanto, J., Prabuwo, A., Abdullah, A., 2013. Real world coordinate from image coordinate using single calibrated camera based on analytic geometry. In: Noah, S., Abdullah, A., Arshad, H., Abu Bakar, A., Othman, Z., Sahran, S., Omar, N., Othman, Z. (Eds.), *Soft Computing Applications and Intelligent Systems*. Springer Berlin Heidelberg, pp. 1–11. https://doi.org/10.1007/978-3-642-40567-9_1.
- Siswanto, J., Prabuwo, A.S., Abdullah, A., 2014a. Volume measurement algorithm for food product with irregular shape using computer vision based on Monte Carlo method. *Journal of ICT Research and Applications* 8 (1), 1–17.
- Siswanto, J., Prabuwo, A.S., Abdullah, A., Idrus, B., 2014b. Monte Carlo method with heuristic adjustment for irregularly shaped food product volume measurement. *Sci. World J.* 10 <https://doi.org/10.1155/2014/683048>, 2014.
- Soltani, M., Omid, M., Alimardani, R., 2015. Egg volume prediction using machine vision technique based on pappus theorem and artificial neural network. *J. Food Sci. Technol.* 52 (5), 3065–3071. <https://doi.org/10.1007/s13197-014-1350-6>.
- Su, Q., Kondo, N., Li, M., Sun, H., Al Riza, D.F., 2017. Potato feature prediction based on machine vision and 3D model rebuilding. *Comput. Electron. Agric.* 137 (Suppl. C), 41–51. <https://doi.org/10.1016/j.compag.2017.03.020>.
- Vivek Venkatesh, G., Iqbal, S.M., Gopal, A., Ganesan, D., 2015. Estimation of volume and mass of axis-symmetric fruits using image processing technique. *Int. J. Food Prop.* 18 (3), 608–626. <https://doi.org/10.1080/10942912.2013.831444>.
- Wang, T.Y., Nguang, S.K., 2007. Low cost sensor for volume and surface area computation of axis-symmetric agricultural products. *J. Food Eng.* 79 (3), 870–877. <https://doi.org/10.1016/j.jfoodeng.2006.01.084>.
- Wang, W., Li, C., 2014. Size estimation of sweet onions using consumer-grade RGB-depth sensor. *J. Food Eng.* 142 (Suppl. C), 153–162. <https://doi.org/10.1016/j.jfoodeng.2014.06.019>.
- Weir, M.D., Thomas, G.B., Hass, J., 2010. *Thomas' Calculus*, twelfth ed. Addison-Wesley, Boston.
- Widiari, M., Santoso, L.P., Siswanto, J., 2019. Computer vision system in measurement of the volume and mass of egg using the disc method. *IOP Conf. Ser. Mater. Sci. Eng.* 703 (1), 012050 <https://doi.org/10.1088/1757-899x/703/1/012050>.
- Zavala de Paz, J.P., Bucio Castillo, F.J., Anaya Rivera, E.K., Isaza Bohorquez, C.A., Castillo Velásquez, F.A., Rizzo Sierra, J.A., 2021. Estimating volume of the tomato fruit by 3D reconstruction technique. *Comput. Syst.* 25 (4).
- Zhang, W., Wu, X., Qiu, Z., He, Y., 2016. A novel method for measuring the volume and surface area of egg. *J. Food Eng.* 170, 160–169. <https://doi.org/10.1016/j.jfoodeng.2015.08.025>.
- Zhou, P., Zheng, W., Zhao, C., Shen, C., Sun, G., 2009. Egg volume and surface area calculations based on machine vision. In: Zhao, C., Li, D. (Eds.), *Computer and Computing Technologies in Agriculture II*. Springer Boston, pp. 1647–1653. https://doi.org/10.1007/978-1-4419-0213-9_15.
- Ziaratban, A., Azadbakht, M., Ghasemnezhad, A., 2017. Modeling of volume and surface area of apple from their geometric characteristics and artificial neural network. *Int. J. Food Prop.* 20 (4), 762–768. <https://doi.org/10.1080/10942912.2016.1180533>.



Volume 334, December 2022

ISSN 0260-8774

journal of food engineering





ScienceDirect

Journal of Food Engineering

Supports open access

8.8

CiteScore

5.354

Impact Factor

Submit your article

Menu

Search in this journal

Latest
issue

Volume 333

In progress • November 2022

About the journal

The journal publishes original research and review papers on any subject at the interface between **food** and **engineering**, particularly those of relevance to **industry**, including:

Engineering properties of foods, **food physics** and **physical chemistry**; processing, measurement, control, packaging, storage ...

[View full aims & scope](#)[↗ International Society of Food Engineering \(ISFE\)](#)

2.2 weeks

Time to First Decision

4.1 weeks

Review Time

0.8 weeks

Publication Time

[View all insights](#)Co-Editors in Chief | [View full Editorial Board](#)

Prof. Dr. Ferruh Erdogdu, PhD

Ankara University Department of Food Engineering, Ankara, Turkey

FEEDBACK



ScienceDirect

Journal of Food Engineering

Supports *open access*

8.8

CiteScore

5.354

Impact Factor

Submit your article ↗

Menu

Search in this journal

Aims and scope

Editorial board

News

Announcements

Conferences

Editorial board

Co-Editors in Chief

Prof. Dr. Ferruh Erdogdu, PhD

Ankara University Department of Food Engineering, Ankara, Turkey

Food Processing, Mathematical modelling, Computational Heat Transfer/Fluid Dynamics, Innovative Food Processing

[View full biography](#)



Professor R. Paul Singh, PhD

University of California Davis Department of Biological and Agricultural Engineering, Davis, California, United States of America

Food engineering, Computational modeling, Sustainability in food processing, Food bioaccessibility during digestion

[View full biography](#)

FEEDBACK

Editors



Professor Bhesh Bhandari, PhD

University of Queensland School of Agriculture and Food Sciences, Saint Lucia, Queensland, Australia

Food Materials Science and Engineering, Food Process Engineering, Food Physical Properties

[View full biography](#)

Dr. Judith Evans

London South Bank University, Dept. of Urban Engineering, Bristol, United Kingdom

Professor Mukund Karwe

Rutgers The State University of New Jersey, New Brunswick, New Jersey, United States of America



Professor Shyam S. Sablani, PhD

Washington State University Department of Biological Systems Engineering, Pullman, Washington, United States of America

Packaging, Food materials science, Reaction kinetics, Physical properties, Thermal processing

[View full biography](#)



Prof. Dr. Susana E. Zorrilla, PhD

Universidad Nacional del Litoral, Santa Fe, Argentina

Heat transfer, Mass transfer, Mathematical modeling, Physical properties of foods

[View full biography](#)

Editorial Board Members



Professor Benu Adhikari, PhD

RMIT University School of Science, Melbourne, Australia

Food material science, Food proteins, Polyphenols, Food powders, Future foods



FEEDBACK 



Professor Lilia M. Ahrné, PhD

Copenhagen University Department of Food Science, Frederiksberg, Denmark

Food Process technology, non-thermal, membrane filtration, powder technology, structure technologies, 3D food printing

[View full biography](#)

Dr. Jose Manuel Barat

Polytechnic University of Valencia, Valencia, Spain

Dr. Jirí Blahovec

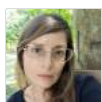
Czech University of Life Sciences Prague Department of Physics, Praha, Czechia



Assoc. Professor Gail Bornhorst, Ph.D

University of California Davis, Davis, California, United States of America

Food digestion, physical properties, food breakdown, mixing



Assist. Prof. Chiara Cevoli, PhD

University of Bologna Department of Agri-Food Sciences and Technologies, Bologna, Italy

Food processing simulation, hyperspectral imaging, spectroscopy, artificial neural network, physical properties



Professor Xiao Dong Chen, PhD

Soochow University, School of Chemical and Environmental Engineering, Suzhou, China

In-Vitro GIT technologies, Drying, Fouling and Cleaning, Powder Technology, Bioinspired Chemical Engineering

Professor Munir Cheryan

University of Illinois Urbana-Champaign, Champaign, Illinois, United States of America

Biofuels, downstream processing, membrane technology

Dr. Mohammed Farid

The University of Auckland, Auckland, New Zealand

Professor Kostadin Fikiin

FEEDBACK

Technical University of Sofia, Sofia, Bulgaria

[View full biography](#)

Professor Denis Flick

Institute of Life and Environmental Sciences and Industries, Paris, France

Professor Peter Fryer

University of Birmingham, Birmingham, United Kingdom

[View full biography](#)



Professor Claire Gaiani, PhD

Université de Lorraine, Department LIBio (Laboratory of Biomolecules Engineering), VANDOEUVRE CEDEX, France

Food powders, Food bioactives, Food surface characterization, Food functional properties, Encapsulation

[View full biography](#)

Professor Miguel Angel Garcia-Alvarado

Technological Institute of Veracruz, Veracruz, Mexico

Professor Gustavo F. Gutiérrez-López

National Polytechnic Institute, Ciudad de Mexico, Mexico

Professor Richard Hartel

University of Wisconsin-Madison, Madison, Wisconsin, United States of America

Professor Jozef L. Kokini, PhD

Purdue University, West Lafayette, Indiana, United States of America



Professor Alain Le Bail, PhD

Process Engineering for Environment and Food Processing, St Nazaire, France

Refrigeration, Freezing, Baking, Phase change, Food quality

[View full biography](#)



Assoc. Professor Yvan Llave Perez, PhD

FEEDBACK

Tokyo University of Marine Science and Technology, Minato-Ku, Japan

Food Processing/Engineering,Mathematical modeling,Dielectric/electric properties,Thermal processing,Electro-processing technologies

Assist. Prof. Francesco Marra

University of Salerno Department of Industrial Engineering, Fisciano, Italy

[View full biography](#)

Professor Rodolfo Mascheroni

National University of La Plata, La Plata, Argentina

Professor Brian McKenna

University College Dublin, Dublin, Ireland

Professor Keshavan Niranjana

University of Reading, Reading, United Kingdom

Food Bioprocessing

Dr. Laura Otero

Spanish Scientific Research Council, Madrid, Spain

Food Science and Technology

Professor Robert Y Peng

HungKuang University, Shalu, Taiwan

Office Tel.: +886-4-26318652-ext 5625 (available on Wednesday and Thursday only)

Dr. Emmanuel Purlis, PhD

National Scientific and Technical Research Council, Buenos Aires, Argentina

Food process engineering ; Transport phenomena ; Physics-based modelling and simulation ; Multiphysics

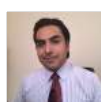


Professor Hosahalli Ramaswamy, PhD

McGill University Department of Food Science and Agricultural Chemistry, Sainte-Anne-de-Bellevue, Quebec, Canada

Food Processing / Engineering, Novel, Technologies, Food Quality and Safety, Process Modeling, Thermo-physical Properties

[View full biography](#)



FEEDBACK 

Dr. Irving Ruiz-López, PhD

Meritorious Autonomous University of Puebla Faculty of Chemical Engineering, Puebla, Mexico

Heat and Mass Transfer, Dehydration, Mathematical modeling, Image Analysis, Food Processing



Professor Fabrizio Sarghini, PhD

University of Napoli Federico II Department of Agriculture, Portici, Italy

Modeling , micro-encapsulation, heat transfer, extrusion, process optimization

Professor Denise Simatos

Professor Ricardo Simpson

Federico Santa Maria Technical University, Valparaiso, Chile

Dr. Juming Tang

Washington State University, Pullman, Washington, United States of America

Dr. Petros Taoukis

National Technical University of Athens, Zografos, Greece

Food science and technology, food engineering



Professor Fidel Toldrá, PhD

Instituto de Agroquímica y Tecnología de Alimentos (CSIC), Valencia, Spain

Enzymology, Proteomics, Peptide chemistry, Meat science

[View full biography](#)

Professor Gilles Trystram

AgroParisTech Massy Centre, Massy, France

Dr. Pieter Verboven

KU Leuven Association, Leuven, Belgium

[View full biography](#)

Dr. Jorge Welte-Chanes

Consortium of the Technological and Higher Education Institute of Monterrey, Monterrey, Mexico

FEEDBACK 

All members of the Editorial Board have identified their affiliated institutions or organizations, along with the corresponding country or geographic region. Elsevier remains neutral with regard to any jurisdictional claims.



Copyright © 2022 Elsevier B.V. or its licensors or contributors.
ScienceDirect® is a registered trademark of Elsevier B.V.





ScienceDirect

Journal of Food Engineering

Supports open access

8.8

CiteScore

5.354

Impact Factor

Submit your article ↗

Menu

Search in this journal

Volume 333

In progress (November 2022)

This issue is in progress but contains articles that are final and fully citable.

[Download full issue](#)[Previous vol/issue](#)[Next vol/issue](#)

Receive an update when the latest issues in this journal are published

[Sign in to set up alerts](#)

Papers

Research article • Full text access

A rapid and accurate computer vision system for measuring the volume of axi-symmetric natural products based on cubic spline interpolation

Joko Siswanto, Endah Asmawati, Muhammad Z.F.N. Siswanto

Article 111139

[Download PDF](#) [Article preview](#)

Research article • Full text access

Analysis of the collision-damage susceptibility of sweet cherry related to environment temperature: A numerical simulating method

Xuewei Han, Ying Liu, Fideline Tchuenbou-Magaia, Zhiguo Li, ... Bangxin Li

Article 111140

[Download PDF](#) [Article preview](#)

Review

FEEDBACK

Review article ● Full text access

Improved encapsulation capacity of casein micelles with modified structure

Xiuju Wang, Zhengtao Zhao

Article 111138

[Download PDF](#) Article preview 

[< Previous vol/issue](#)

Next vol/issue [>](#)

ISSN: 0260-8774

Copyright © 2022 Elsevier Ltd. All rights reserved



Copyright © 2022 Elsevier B.V. or its licensors or contributors.
ScienceDirect® is a registered trademark of Elsevier B.V.

 RELX™

FEEDBACK 



Source details

Journal of Food Engineering

Scopus coverage years: from 1982 to Present

Publisher: Elsevier

ISSN: 0260-8774

Subject area: Agricultural and Biological Sciences: Food Science

Source type: Journal

CiteScore 2020

8.8



SJR 2020

1.291



SNIP 2020

1.727



[View all documents >](#)

[Set document alert](#)

[Save to source list](#) [Source Homepage](#)

[CiteScore](#) [CiteScore rank & trend](#) [Scopus content coverage](#)

i Improved CiteScore methodology



CiteScore 2020 counts the citations received in 2017-2020 to articles, reviews, conference papers, book chapters and data papers published in 2017-2020, and divides this by the number of publications published in 2017-2020. [Learn more >](#)

CiteScore 2020

$$8.8 = \frac{11,903 \text{ Citations 2017 - 2020}}{1,347 \text{ Documents 2017 - 2020}}$$

Calculated on 05 May, 2021

CiteScoreTracker 2021

$$10.5 = \frac{14,129 \text{ Citations to date}}{1,351 \text{ Documents to date}}$$

Last updated on 06 April, 2022 • Updated monthly

CiteScore rank 2020

Category	Rank	Percentile
Agricultural and Biological Sciences	#15/310	95th
Food Science		

[View CiteScore methodology >](#) [CiteScore FAQ >](#) [Add CiteScore to your site](#)

About Scopus

- What is Scopus
- Content coverage
- Scopus blog
- Scopus API
- Privacy matters



Language


- 日本語に切り替える
- 切换到简体中文
- 切换到繁體中文
- Русский язык

Customer Service

- Help
- Tutorials
- Contact us

ELSEVIER

[Terms and conditions](#)  [Privacy policy](#) 

Copyright © Elsevier B.V . All rights reserved. Scopus® is a registered trademark of Elsevier B.V.
We use cookies to help provide and enhance our service and tailor content. By continuing, you agree to the use of cookies.

